CrossMark

A tunable single-polarization photonic crystal fiber filter based on surface plasmon resonance

Shuhuan Zhang[1] · Jianshe Li[1] · Shuguang Li[1] · Qiang Liu[1] · Yingchao Liu[1] · Zhen Zhang[1] · Yujun Wang[1]

Abstract

A tunable single polarizing filter is proposed by selectively coating gold film on the air holes of photonic crystal fiber (PCF). The polarization properties of the PCF filter are evaluated by the finite-element method. Simulation results show that the loss of y-polarized core mode at 1250 and 1550 nm is 136.23 and 839.73 dB/cm, respectively. Furthermore, we innovatively combine stable modulation with flexible modulation. To be specific, the resonance wavelengths are slowly controlled in a small wavelength range by altering the diameter of the air-hole-coated gold film, while the resonance wavelengths are flexibly controlled in a wide wavelength range by altering the thickness of the gold film or the diameter of the small air holes. When the length of the PCF is 500 μm, the bandwidth of extinction ratio greater than − 20 dB is only 60 nm at the communication window of 1550 nm. It is beneficial to fabricate a narrow-band polarization filter.

1 Introduction

In recent years, photonic crystal fibers (PCFs), which are also known as holey fibers and microstructure optical fibers, have attracted more and more attention due to their unique advantages, such as low or high nonlinearity [1, 2], high birefringence [3], low loss [4], large mode area [5], and so on. In addition, the optical properties of PCFs can be greatly improved by selectively filling or coating different materials in the air holes, such as oil [6], liquid [7], liquid crystal [8], metal [9], and so on. In a metal coated or filled PCF, the air holes of the coated metal film or filled metal wire can be used as the core of the defect. When the incident light transmission mode in the fiber core matches with the surface plasmon mode, the light in the fiber core mode is coupled to the defect mode; thus, the surface plasmon resonance [10] is formed. Furthermore, due to the surface plasmon resonance effect, the confinement loss of the incident light in the two orthogonal polarization directions varies considerably.

Accordingly, this property can be used in the development of polarization filter.

In 2007, a selective coating technique for PCFs was demonstrated by Zhang et al. [11], whereby a polarization filter based on PCF is proposed, and silver film was selectively coated on the air holes of PCF for the first time. In 2008, Lee et al. [12] proposed a new method for selectively filling gold nanowires in PCF. The results show that the PCF filled with metal has obvious polarization transmission characteristics, which is in good agreement with the finite-element simulation results. In 2015, Chen et al. [13] proposed an ultra-wideband polarization filter based on depositing the gold film on the polished surface of PCF and found surface plasmons and photons generate multiple resonances. In 2017, Zhang et al. [14] designed a simple polarization filter based on a single air hole coated gold film of PCF. The peak loss in y-polarization direction is 2138.34 dB/cm at the 1.31 μm communication window. However, the confinement loss in x-polarization direction is very low.

In this paper, we propose a tunable single-polarization filter based on a single air hole coated gold film in PCF. The polarization characteristics of our proposed PCF filter are calculated by the finite-element method (FEM) [15]. Simulation results show that the peak losses in y-polarization direction are 136.23 and 839.73 dB/cm at the wavelength 1.25 and 1.55 μm, respectively, while the confinement losses are very low in x-polarization direction. Moreover, the loss peak 1 can be slowly modulated over a small wavelength range by

✉ Jianshe Li
    jianshelee@ysu.edu.cn

[1] State Key Laboratory of Metastable Materials Science and Technology and Key Laboratory for Microstructural Material Physics of Hebei Province, School of Science, Yanshan University, Qinhuangdao 066004, People's Republic of China

changing the size of large air holes. In addition, the loss peak 1 can be flexibly modulated over a wide wavelength range by changing the thickness of the gold film or the size of the small air holes. Meanwhile, the polarization characteristics are compared by coating gold film or filling metal wire in the air hole of the PCF. It can be concluded that the gold-plating has a more pronounced effect on the polarization properties of PCF. When the length of the PCF is 500 μm, the extinction ratio is better than −20 dB, and the effective filtering wavelength range is just from 1.52 to 1.58 μm. Therefore, our designed PCF can be applied to tunable narrow-band polarization filter.

2 Geometry of a PCF filter

Figure 1a shows the cross section of our proposed PCF. The blue part is the background material (silica) of the PCF. Many air holes in the space are arranged in a hexagonal lattice, and the distance between each air hole is represented by Λ. The diameter of the white air holes is d_1, and the diameter of the six green air holes is represented by d_3. As we know, the effective refractive index of the air is equal to 1. The purple air hole diameter d_2, and coated with gold film. The thickness of the gold film is expressed by t. The fiber cladding consists of four layers of air holes that effectively confine the light within the core. A gold-coated large air hole is introduced above the core, destroying the symmetry of the structure and creating birefringence, which clearly distinguishes the loss in the x and y polarization directions. In addition, there are six small air holes around the large air hole coated with gold film, and by changing the size of small air holes, the coupling between the surface plasmon mode and the core mode can be easily adjusted, so that the surface plasmon resonance occurs more easily.

As shown in Fig. 1b, the finite-element method (FEM) mesh is used to discrete the physical field for calculation. We select the radio frequency (RF) module in the COMSOL Multiphysics software for numerical simulation. In the computational domain settings, we set the outermost ring as the perfectly matched layer (PML), whose type is "cylindrical". PML is a very good absorption boundary condition which can absorb radiant energy of incident light at various angles and not reflect energy. In the outer boundary of the PCF settings, the scattering boundary condition (SBC) is taken as the outer boundary of the PML, which further reduces the reflection energy. Therefore, we can obtain more accurate mode loss characteristics. In the PCF-free mesh parameter settings, we use the predefined mesh size types as "coarse". The cross section is discretized by triangular subdomains and the total number of mesh elements is 22,582. Thus, the simulation results are balanced between the simulation speed and the accuracy.

In this structure, the background material is pure silica and the dispersion relationship is calculated by the Sellmeier equation [16]. In addition, we calculate the dielectric constant of the gold film by Drude–Lorentz model [17]. We take into account the propagation feature of PCF filters is greatly affected by the confinement loss, which can be defined by the following formula [18]:

$$\alpha(\beta_1, \beta_2) = 8.686 \times \frac{2\pi}{\lambda} \mathrm{Im}(n_{\mathrm{eff}}) \times 10^4, \tag{1}$$

where λ expresses the wavelength of light and $\mathrm{Im}(n_{\mathrm{eff}})$ expresses the imaginary part of effective refractive index. β_1 and β_2 are expressed as x- and y-polarized modes, respectively. Here, we specify the unit of loss is dB/cm, and the unit of wavelength is μm. Under different structural parameters, phase matching is achieved when the transmission constants of the core mode and surface plasmon mode at a certain wavelength are the same. The "certain wavelength"

Fig. 1 **a** Cross-sectional schematic of the proposed PCF. **b** FEM mesh and scattering boundary condition for computation
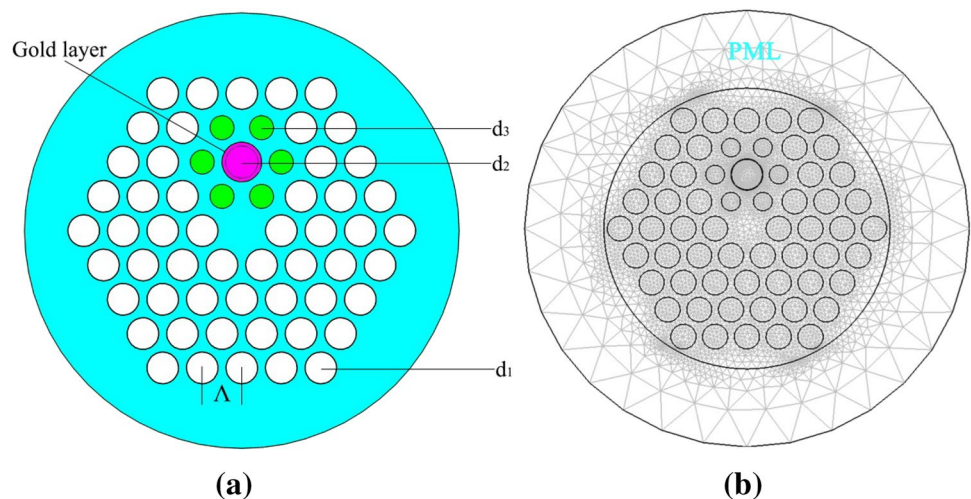
is the resonance wavelength that corresponds to the confinement loss peak. In this case, the light intensity in the core mode will be greatly weakened and transferred to the surface of the gold film. That is, the light field energy is transferred from the core mode to the surface plasmon mode, resulting in resonance phenomenon.

3 Numerical result and analysis

To facilitate the analysis of the dispersion relation (effective refractive index and confinement loss) between the core mode and the SPP mode, and the distribution of electric field intensity under different resonant wavelengths (1550 and 1250 nm), we combine the dispersion relation with the electric field distribution in Fig. 2. Among them, Fig. 2c–j shows the distribution of electric field intensity under different resonant wavelengths. The red arrow in the figure shows the direction of the electric field in different modes. As shown in Fig. 2a, b, the black solid line and dotted line represent the *y*-polarized and *x*-polarized core modes, respectively. The blue and red solid lines represent the second-order and third-order SPP modes, respectively. It is obvious that the effective refractive index curve of core mode and SPP mode intersect at the resonance wavelength 1550 and 1250 nm, respectively. Moreover, the wavelengths corresponding to the effective refractive index cross point (phase matching point) coincides with the resonance wavelengths corresponding to the confinement loss. It is easy to see that the losses of the core mode and the SPP mode are not equal at the phase-matching points and are separated from each other. The maximum

value of the loss in the core mode is less than the minimum value of the loss in the SPP mode. In reference [19], this phenomenon is known as incomplete coupling.

As shown in Fig. 2b, at the resonance wavelength 1550 nm, the confinement loss of the *y*-polarized core mode can reach to 839.73 dB/cm, while the loss of the *x*-polarized core mode is very low. At the same time, it can be seen from Fig. 2c that the energy of the *x*-polarized core mode is completely limited to the fiber core and no other energy is coupled to the surface of the gold film. Therefore, no surface plasmon resonance phenomenon was observed. However, in Fig. 2d, the energy of the *y*-polarized core mode is partially limited to the fiber core and the other part of energy is clearly coupled to the surface of the gold film. Therefore, the surface plasmon resonance phenomenon was observed. As a result, the loss of *y*-polarized core mode is much stronger than the *x*-polarized core mode. This is mainly due to a part of the energy transferred from the fiber core to the gold film surface.

In addition, it is obvious in Fig. 2b that the loss of the *y*-polarized second-order SPP modes is much stronger than that of the *y*-polarized core modes. The above phenomena can be explained by comparing the electric field distribution of Fig. 2d, f. The *y*-polarized core mode (d) and the *y*-polarized second-order SPP mode (f) appear very similar in the energy distribution. However, we can see clearly that the *y*-polarized core mode is superior to the *y*-polarized second-order SPP mode in terms of the energy constraint of the fiber core. In other words, the energy in Fig. 2f is more transferred from the fiber core to the gold film surface, so that it has a higher confinement loss. Therefore,

Fig. 2 Relationship between **a** effective refractive index and **b** confinement loss. the electric field distributions of **c** *x*-polarized, **d** *y*-polarized core modes, and **e** *x*-polarized, **f** *y*-polarized second-order SPP modes at the wavelength of 1.55 μm. The electric field distributions of **g** *x*-polarized, **h** *y*-polarized core modes and **i** *x*-polarized, **j** *y*-polarized third-order SPP modes at the wavelength of 1.25 μm. In addition, the PCF parameters are $d_1 = 1.6$ μm, $d_2 = 2.0$ μm, $d_3 = 1.2$ μm, and $t = 25$ nm
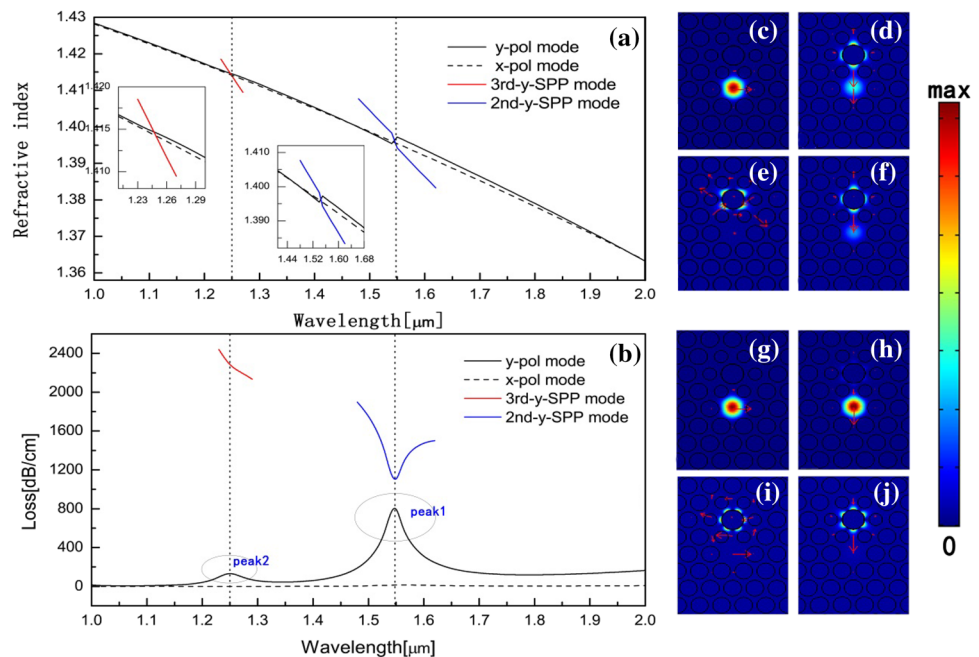
the phenomenon of incomplete coupling is produced. Meanwhile, the simulation results show that the imaginary part of the refractive index of Fig. 2d (0.002385i) is less than Fig. 2f (0.003015i). Therefore, Fig. 2d shows the *y*-polarized core mode and Fig. 2f shows *y*-polarized second-order SPP mode.

Next, at the resonance wavelength 1250 nm, the confinement loss of the *y*-polarized core mode can reach to 136.23 dB/cm, while the loss of the *x*-polarized core mode is low. In Fig. 2g, it can be seen that the energy of the *x*-polarized core mode is completely limited to the fiber core. However, in Fig. 2h, most of the *y*-polarized core mode energy is confined to the fiber core, and only a small fraction of the energy is coupled to the gold film surface. As a result, the loss of *y*-polarized core mode is slightly stronger than the *x*-polarized core mode. This is because the small fraction of the energy transferred from the fiber core to the gold film surface. As shown in Fig. 2b, the loss of the *y*-polarized core mode is not very high. In addition, it is obvious in Fig. 2b that the loss of the *y*-polarized third-order SPP modes is much stronger than that of the *y*-polarized core modes. The above phenomena can be explained by comparing the electric field distribution of Fig. 2h, j. We can see clearly that the energy of the *y*-polarized third-order SPP mode (j) is completely coupled to the surface of the gold film. In other words, Fig. 2j almost all of the energy is transferred from the fiber core to the gold film surface, so that it has a higher confinement loss. Therefore, the phenomenon of incomplete coupling is produced.

In the end, we can find that the *y*-polarized core mode is suppressed and only *x*-polarized core mode can be guided. Therefore, we get the effect of the single-polarization filter.

Table 1 compares the performance of several PCF-based polarization filters. On one hand, Refs. [18, 21] and this work are single air hole-coated gold film, yet Refs. [20, 22, 23] are two air holes coated gold film. In actual operation, single-hole gold plating is easier than double-hole gold-plating. On the other hand, at the communication wavelength of 1550 nm, the value of the confinement loss of 839.73 dB/cm is much higher than the previous reports in Refs. [18, 21], which are 242.89 and 410.04 dB/cm, respectively. It can

be observed that the polarization properties of PCF-based polarization filters we proposed have been significantly optimized and improved.

According to the current manufacturing process, the confinement loss of our proposed PCF is higher than 1 dB/m which is much greater than the material loss of silica. Therefore, the material loss is neglected. Thus, the output power of $P_{\text{out}}(\beta_1, \beta_2)$ is obtained by the equation:

$$P_{\text{out}}(\beta_1, \beta_2) = P_{\text{in}}(\beta_1, \beta_2)\exp\left(-\alpha(\beta_1, \beta_2)\left(\frac{\ln 10}{10}\right)L\right), \quad (2)$$

where $P_{\text{out}}(\beta_1, \beta_2)$ is normalized. Moreover, $P_{\text{in}}(\beta_1, \beta_2)$ is the input power and is considered to 1, the length of PCF is represented by L, and the confinement loss is represented by (β_1, β_2). The extinction ratio (ER) is proposed as [20]:

$$\text{ER} = 10\log_{10}\left(\frac{P_{\text{out}}(\beta_2)}{P_{\text{out}}(\beta_1)}\right). \quad (3)$$

Figure 3a shows the output power of the *x*-polarized mode and *y*-polarized mode at different PCF lengths. As the transmission length increases, the output power in two orthogonal directions decreases obviously. In the wavelength range 1.2–1.3 and 1.5–1.6 μm, the output power of *x*-polarized mode is close to 1, while the output power of *y*-polarized mode is close to 0. In the wavelength range we mentioned above, there is a big gap between the output power in the *x*-polarized and *y*-polarized direction. In other words, we chose the appropriate fiber length to keep the output power in the *x*-polarization direction at a high level, while the output power of *y*-polarization direction is reduced to a small enough. In this way, we can get a fine ER, as shown in Fig. 3b. Figure 3b shows the relationship between ER and different fiber lengths. It can be seen that as the PCF length increases from 300 to 500 μm, the ER is gradually reduced. When the length of the PCF is 500 μm, the extinction ratio is better than −20 dB and the effective filtering wavelength range is only from 1.52 to 1.58 μm. As far as we know, the bandwidth is very narrow. Therefore, it is advantageous to make narrow band filter. Sum up: it is obvious that the

Table 1 Different polarization filters based on PCF are detailed and systematically contrasted

PCF structure and references	Peak loss at 1.55 μm (dB/cm)
The air holes are arranged in a square lattice and the two small holes are deposited by a thin layer of gold (Liu et al. [20])	102.00
Two small air holes are set inside the fiber core, and a single air hole around the core is filled with gold wire (Li et al. [18])	242.89
Two large air holes compressed fiber core (high birefringence), and a single hole coated with gold film (Liu et al. [21])	410.04
The small air hole in the fiber core is filled with pure water, and two air holes are coated with gold film (Jiang et al. [22])	536.25
The air holes are arranged in a rhombic lattice, two air holes near the core are coated with gold layer (Dou et al. [23])	630.20
A single air hole is coated with a layer of gold, surrounded by six small air holes (This work)	839.73

Fig. 3 **a** Output power of *x*-polarized mode and *y*-polarized mode and **b** extinction ratio curve at different PCF lengths, and the PCF parameters are $d_1 = 1.6$ μm, $d_2 = 2.0$ μm, $d_3 = 1.2$ μm, $t = 25$ nm
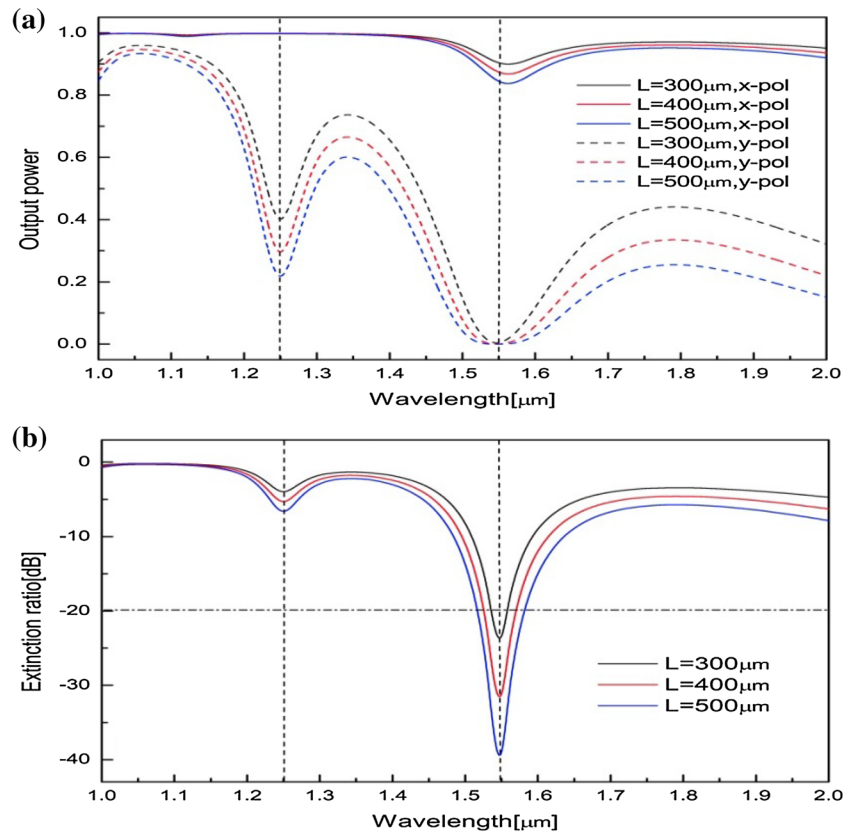

4 Tunable polarization filter

We innovatively combine stable modulation with flexible modulation. The resonance wavelengths are slowly modulated in a small wavelength range (the wavelengths of 1.54–1.57 μm) by altering the diameter of the air hole-coated gold film. In addition, the resonance wavelengths are flexibly modulated in a wide wavelength range (the wavelengths of 1.45–1.74 μm) by altering the diameter of the small air holes or the thickness of the gold film.

In the first place, the resonance wavelengths of the loss peak 1 are slowly modulated in a small wavelength range (1.54–1.57 μm) by altering the diameter of the large air hole. On one hand, as shown in Fig. 4b, with the diameter of the large air hole increases from 1.6 to 1.8 μm, the resonance peak 1 of *y*-polarized core mode causes a red-shift and the value of confinement loss increases from 517 to 803 dB/cm. It is revealed from Fig. 4a that the large air hole diameter increases from 1.6 to 1.8 μm resulting in a real part of the 2-SPP mode refractive index increases. However, it has a weak influence on the dispersion characteristics of the *y*-polarized core mode. Therefore, the *y*-polarized core

mode and 2-SPP mode phase-matching point move to the long-wave direction (red-shift). On the other hand, as shown in Fig. 4b, with the diameter of the large air hole increases from 1.8 to 2.0 μm, the resonance peak 1 of *y*-polarized core mode causes a blue-shift and the value of confinement loss increases from 803 to 839 dB/cm. It is revealed from Fig. 4a that the large air hole diameter increases from 1.8 to 2.0 μm resulting in a real part of the 2-SPP mode refractive index decreases. However, it has a weak influence on the dispersion characteristics of the *y*-polarized core mode. Therefore, the core mode and 2-SPP mode phase-matching point move to the short wave direction (blue-shift). In summary, it can be seen from Fig. 4b that the resonance loss peak 1 of *y*-polarized core mode increases with the diameter of the large air hole. As far as we concerned, the large air hole is coated with gold film, and the thickness of the gold film is constant. However, as the diameter of the large air hole coated with gold film increases, it is closer to the fiber core. This makes it easier to transfer some energy from the core to the surface of the gold film, and eventually resulting in increased confinement loss at the resonance wavelength.

Therefore, we finally came to a conclusion: With the increase of the diameter of the large air holes, the resonance peak 1 has undergone red-shifted and blue-shifted, and the value of peak 1 loss has been increasing.

Fig. 4 a Effective refractive indices of *y*-polarized core modes and 2-SPP modes at different diameters of the large air hole. **b** is the corresponding losses spectra of *y*-polarized core modes, and the PCF parameters are $d_1 = 1.6$ μm, $d_3 = 1.2$ μm, $t = 25$ nm
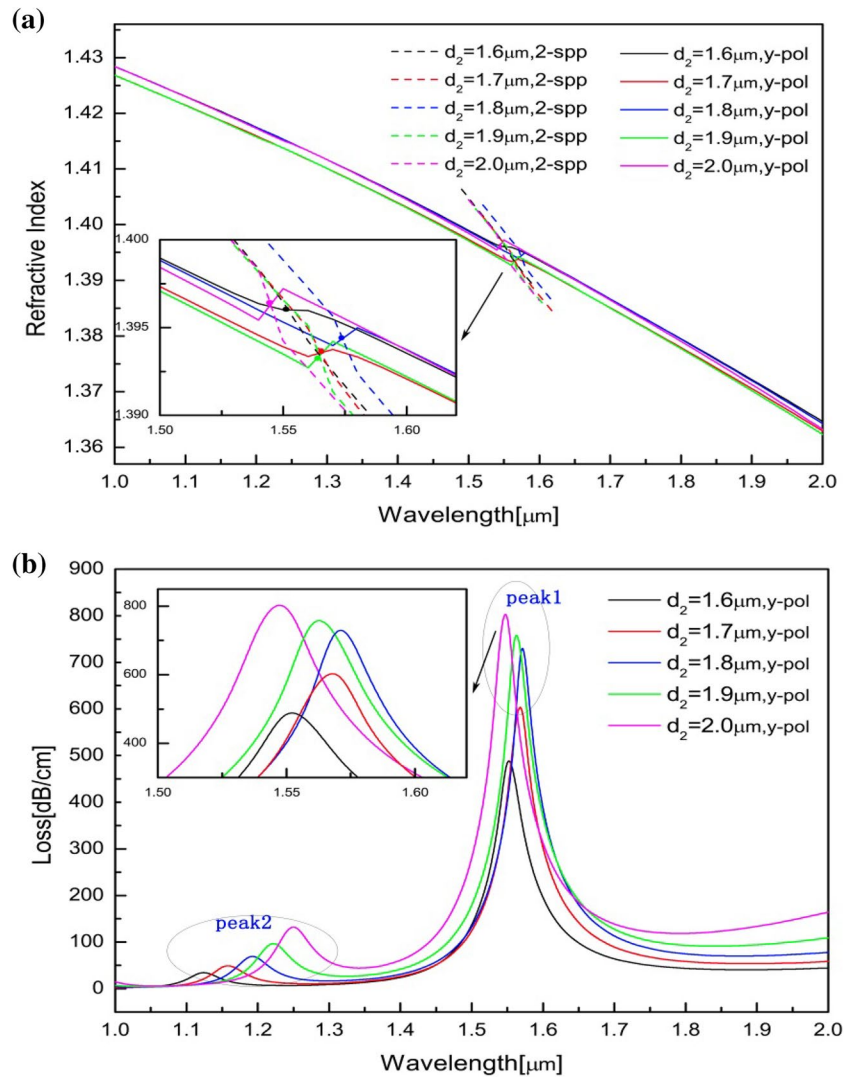
Next, the resonance wavelengths of the loss peak 1 are flexibly modulated in a wide wavelength range (1.45–1.74 μm) by altering the diameter of the small air holes or the thickness of the gold film. Figure 5a, b shows the effect of size of six small air holes to the polarization characteristics of the PCF. It can be seen from Fig. 5b that the loss peak of *y*-polarized core mode experiences a blue-shift as d_3 increases. It is revealed from Fig. 5a that the six small air holes diameter increases from 1.0 to 1.2 μm, resulting in a real part of the 2-SPP mode refractive index decreases. However, it has a weak influence on the dispersion characteristics of the *y*-polarized core mode. Therefore, the core mode and 2-SPP mode phase-matching point move to the short wave direction (blue-shift). In addition, the diameter of the d_3 varies from 1.0 to 1.2 μm, the height of the *y*-polarized loss peak 1 increases, while the height of the *y*-polarized loss peak 2 decreases. As far as we concerned, when d_3 decreases (d_3 is reduced from 1.2 to 1.0 μm), the interaction area between the fiber core and large air hole (d_2)

coated with gold film increases, making the energy between them easier to couple and resulting in a wide range of resonance [wider FWHM (full width at half maximum)]. Then, through the law of conservation of energy, the energy of loss peak 1 is reduced, some of the energy is transferred to the loss peak 2, and the other part of the energy increases the FWHM of resonance peak.

We all know that the surface plasmon waves are very sensitive to the thickness of the gold layer. Figure 5c, d shows the effect of gold film changes on the polarization characteristics of the PCF. When the gold film thickness is 25 nm, the loss peak 1 of *y*-polarized mode is up to 839.73 dB/cm. There is no doubt that the loss peak 1 of *y*-polarized mode experiences a blue-shift and the value of loss peak 1 becomes lower with the increase of the gold film thickness. It is revealed from Fig. 5c that the thicknesses of the gold film increases from 25 to 31 nm resulting in a real part of the 2-SPP mode refractive index decreases. However, it has a weak influence on the dispersion characteristics of the *y*-polarized core mode.
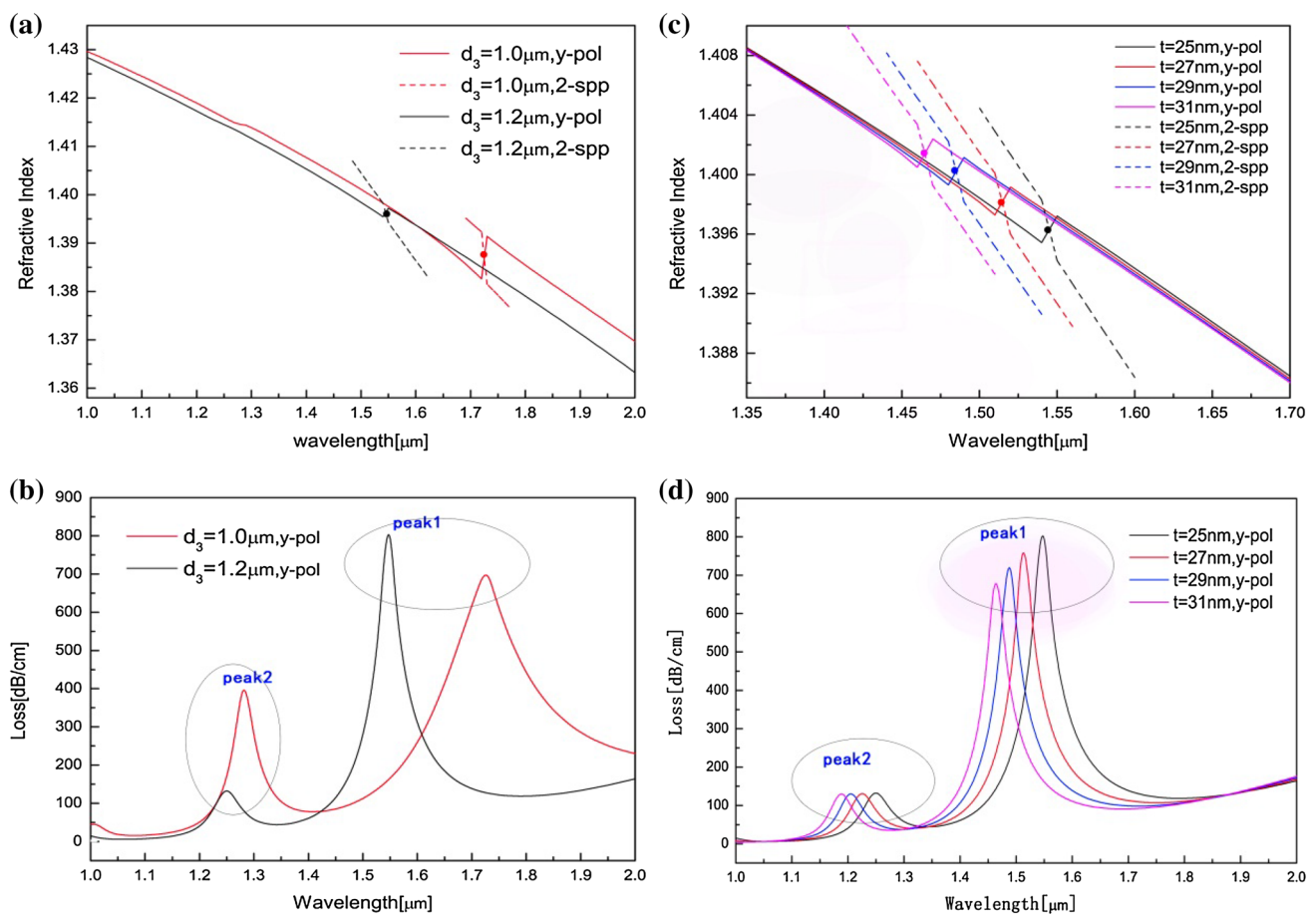
Fig. 5 **a** Effective refractive indices of *y*-polarized core modes and 2-SPP modes at different diameters of the six small air holes. **b** is the corresponding losses spectra of *y*-polarized core modes, and the PCF parameters are $d_1 = 1.6$ μm, $d_2 = 2.0$ μm, $t = 25$ nm. **c** Effective refrac- tive indices of *y*-polarized core modes and 2-SPP modes at different thicknesses of the gold film. **d** is the corresponding losses spectra of *y*-polarized core modes, and the PCF parameters are $d_1 = 1.6$ μm, $d_2 = 2.0$ μm, $d_3 = 1.2$ μm

Therefore, the core mode and 2-SPP mode phase matching point move to the short wave direction (blue-shift). As far as we concerned, when the coated gold film is too thick, the loss of *y*-polarized core mode will be correspondingly reduced. This is mainly due to that the gold coating is too thick, and the electric field is difficult to penetrate. This makes the excited SPR effect weakened, eventually leads to a decrease in the resonant peak.

All in all, a tunable PCF polarization filter is proposed. We innovatively combine stable modulation with flexible modulation. The analysis results show that the designed PCF will play a significant role in the development of tunable polarization filter.

5 Comparison of different filling methods

To analyze and compare the performance of the polarization filter, we proposed that we adopt different filling methods and different filled metals in the large air hole.

The comparison of the confinement losses of gold-coated and without gold-coated large air hole is shown in Fig. 6. The PCF optimal structure parameters are $d_1 = 1.6$ μm, $d_2 = 2.0$ μm, $d_3 = 1.2$ μm, and $t = 25$ nm. On one hand, for the PCF coated with gold film, the loss of *y*-polarized core mode can reach 136.23 dB/cm at 1250 nm and 839.73 dB/cm at 1550 nm. In addition, the loss of the
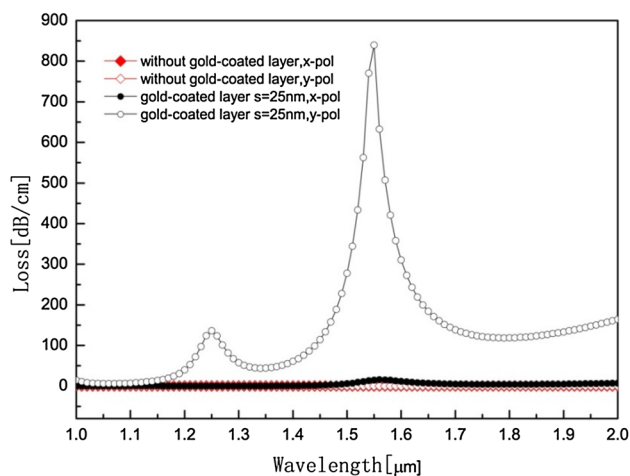
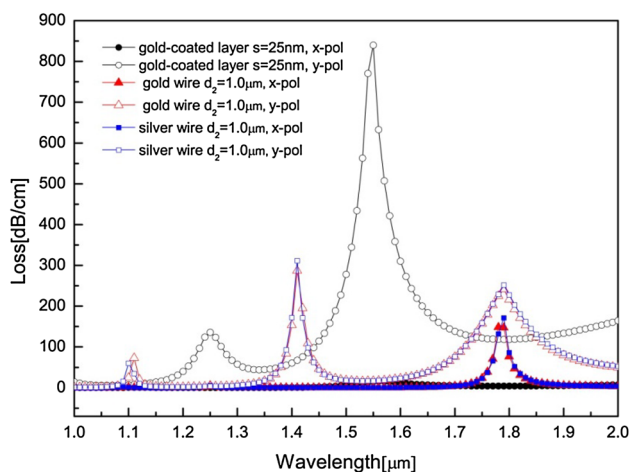**Fig. 6** Comparison of the losses between gold-coated and without gold-coated PCF

Fig. 7 Contrast of losses of the PCFs with metal wire filling and a gold-coated layer

y-polarized core mode is stronger than that of the x-polarized core mode. On the other hand, for the PCF without coated gold film, the x-polarized and y-polarized core modes are below 0.01 dB/cm. We all know that surface plasmon waves are very sensitive to the thickness of the gold layer. The energy of the y-polarized core mode (gold-coated) has been coupled to the surface of the coated gold film, so that it has a higher confinement loss. Undoubtedly, by coating gold film in the large air hole, the polarization property of the PCF is greatly improved.

The comparison of confinement losses of the PCF with a metal-filled wire (gold or silver [24]) and a gold-coated layer is shown in Fig. 7. It is revealed from Fig. 7 that the gold film is coated in the large air hole, and the confinement loss in the y polarization direction can reach 839.73 dB/cm,

which is much higher than that the metal-filled wire (gold or silver) in the large air hole. We all know that surface plasmon wave is extremely susceptible to the change of gold film thickness. The electric field is difficult to penetrate when the gold film is very thick, which weakens the excited SPR effect and eventually reduces the loss peak. In addition, we have found that the difference of the loss characteristics of the PCF filling with gold and silver wire, respectively, is not very clear.

In summary, we can conclude that the gold-coated layer has more remarkable influence on the polarization feature of PCF. Meanwhile, unlike other metal materials, gold is chemically inert and does not be oxidized easily.

6 Conclusion

A tunable single-polarization filter with gold-coated single air hole is put forwarded. The polarization characteristics of the PCF are analyzed by the finite element method. It also should be noted that the loss of y-polarized mode reaches to a highest value of 839.73 dB/cm at the wavelength of 1.55 μm. In contrast, the loss of x-polarized mode is just 14.7 dB/cm. Moreover, the loss peak 1 can be slowly modulated over a small wavelength range. In addition, the loss peak 1 can also be flexibly modulated over a wide wavelength range. We also analyzed the effect of the metal-filled wire and gold-coated layer on the loss of PCFs. The results showed that the gold-coated layer had more obvious influence on the polarization properties of PCF. When the PCF length is set to 500 μm, the bandwidth of extinction ratio greater than −20 dB is very narrow. The above results show that it can be widely used as a PCF polarization filter with excellent performance in the field of communication transmission.

References

1. J. Limpert, A. Liem, M. Reich, T. Schreiber, S. Nolte, H. Zellmer, A. Tünnermann, Low-nonlinearity single-transverse-mode ytterbium-doped photonic crystal fiber amplifier. Opt. Express **12**(7), 1313–1319 (2004)
2. J. Park, J. Kim, S. Lee, S. Kim, K. Oh, Ultra-flattened dispersion and high nonlinearity in a square lattice photonic crystal fiber. In: Optoelectronics and communications conference. IEEE, 7P (42), pp. 340–341 (2010)
3. S. Yuhsien, Y. Chau, H. Yeh, L. Shen, T. Yang, D. Tsai, High birefringence photonic crystal fiber with a complex unit cell of

asymmetric elliptical air hole cladding. Appl. Opt. **46**(22), 5276–5281 (2007)

4. K. Suzuki, H. Kubota, S. Kawanishi, Optical properties of a low-loss polarization-maintaining photonic crystal fiber. Opt. Express **9**(13), 676–680 (2001)

5. J.R. Folkenberg, M.D. Nielsen, N.A. Mortensen, C. Jakobsen, H.R. Simonsen, Polarization maintaining large mode area photonic crystal fiber. Opt. Express **12**(5), 956–960 (2004)

6. D. Rativa, B. Vohnsen, Wavefront sensing with an oil-filled photonic crystal fiber. In: Frontiers in optics (OSA Publishing, 2012)

7. W. Qian, C. Zhao, Y. Wang, C. Chan, S. Liu, W. Jin, Partially liquid-filled hollow-core photonic crystal fiber polarizer. Opt. Lett. **36**(16), 3296–3298 (2011)

8. A. Lorenz, H.S. Kitzerow, A. Schwuchow, J. Kobelke, H. Bartelt, Photonic crystal fiber with a dual-frequency addressable liquid crystal: behavior in the visible wavelength range. Opt. Express **16**(23), 19375–19381 (2008)

9. B. Sun, M.-Y. Chen, Y.-K. Zhang, J. Zhou, Polarization-dependent coupling characteristics of metal-wire filled dual-core photonic crystal fiber. Opt. Quantum Electron. **47**(2), 441–451 (2015)

10. Z. Tan, X. Hao, Y. Shao, Y. Chen, X. Li, P. Fan, Phase modulation and structural effects in a D-shaped all-solid photonic crystal fiber surface plasmon resonance sensor. Opt. Express **22**(12), 15049–15063 (2014)

11. X. Zhang, R. Wang, F.M. Cox, B.T. Kuhlmey, M.C.J. Larg, Selective coating of holes in microstructured optical fiber and its application to in-fiber absorptive polarizers. Opt. Express **15**(24), 16270–16278 (2007)

12. H.W. Lee, M.A. Schmidt, H.K. Tyagi, L. Prill Sempere, P.S.J. Russell, Polarization-dependent coupling to plasmon modes on submicron gold wire in photonic crystal fiber. Appl. Phys. Lett. **93**(11), 111102-1–111102-3 (2008)

13. H. Chen, S. Li, G. An, J. Li, Z. Fan, Y. Han, Polarization splitter based on d-shaped dual-core photonic crystal fibers with gold film. Plasmonics **10**(1), 57–61 (2015)

14. W. Zhang, S. Lou, X. Wang, A polarization filter based on a novel photonic crystal fiber with a gold-coated air hole by using surface plasmon resonance. Plasmonics **13**(2), 365–371 (2018)

15. Q. Liu, S. Li, C. Dou, X. Wang, Defected-core photonic crystal fiber magnetic field sensor based on Sagnac interferometer. Appl. Phys. B **123**(3), 65 (2017)

16. X. Yang, Y. Lu, B. Liu, J. Yao, Polarization characteristics of high-birefringence photonic crystal fiber selectively coated with silver layers. Plasmonics **13**, 1035–1042 (2018)

17. X. Feng, H. Du, S. Li, Y. Zhang, Q. Liu, X. Gao, A broadband core shift polarization filter based on photonic crystal fiber with a big gold-coated air hole. Opt. Quantum Electron. **49**(7), 235 (2017)

18. M. Li, Lu Peng, G. Zhou, B. Li, Z. Hou, C. Xia, Design of photonic crystal fiber filter with narrow width and single-polarization based on surface plasmon resonance. IEEE Photonics J. **9**(3), 5700108 (2017)

19. Q. Liu, S. Li, H. Chen, Two kinds of polarization filter based on photonic crystal fiber with nanoscale gold film. IEEE Photonics J. **7**(1), 2700210 (2015)

20. Q. Liu, S. Li, H. Li, J. Zi, W. Zhang, Z. Fan, G. An, Y. Bao, Broadband single-polarization photonic crystal fiber based on surface plasmon resonance for polarization filter. Plasmonics **10**(4), 931–939 (2015)

21. Q. Liu, S. Li, J. Li, H. Chen, Z. Fan, G. An, H. Li, J. Zi, Photonic crystal fiber polarization filter basedon coupling between core mode and spp mode. Plasmonics **11**, 857–863 (2016)

22. L. Jiang, Y. Zheng, L. Hou, K. Zheng, J. Peng, Surface plasmon induced polarization filter of the gold-coated photonic crystal fiber with a liquid core. Opt. Fiber Technol. **23**, 42–47 (2015)

23. C. Dou, X. Jing, S. Li, Q. Liu, J. Bian, A photonic crystal fiber polarized filter at 1.55 μm based on surface plasmon resonance. Plasmonics **11**, 1163–1168 (2016)

24. A.K. Sharma, Rajan, B.D. Gupta, Influence of dopants on the performance of a fiber optic surface plasmon resonance sensor. Opt. Commun. **274**(2), 320–326 (2007)